06.1;06.5;05.1

Strengthening of polycrystalline ice by silica nanoparticles

© Yu.I. Golovin[1,2], A.A. Samodurov[1], V.V. Rodaev[1], A.I. Tyurin[1], D.Yu. Golovin[1], S.S. Razlivalova[1], V.M. Buznick[1,2]

[1] Tambov State University, Tambov, Russia
[2] Moscow State University, Moscow, Russia
E-mail: yugolovin@yandex.ru, nano@tsutmb.ru

Received February 27, 2023
Revised April 6, 2023
Accepted April 6, 2023

Ice as a construction material has a number of advantages in the Arctic. It is a local, renewable, ecologically safe resource, and it does not require supplying from the mainland. However, mechanical characteristics of natural ice are rather low. The potential of known techniques of ice strengthening employing reinforcement by microfibers or macroscopic components is limited. The paper describes strengthening of the ice matrix using nanodisperse silica particles. Six-fold reduction of grain size induced by adding 10% wt of SiO_2 nanoparticles results in 2.5 times increase in strength limit in the uniaxial compression test and more than an order of magnitude increase in fracture energy.

Keywords: polycrystalline ice, mechanical properties, grain structure.

DOI: 10.61011/TPL.2023.06.56370.19542

Large-scale development of the Arctic region planned in the framework of the RF Development Strategy needs large amounts of low-cost construction materials not liable to supplying from the „mainland". Under the Far North conditions, the most available of those materials are water, snow, ice, and other geomaterials. Ice and snow possess a lot of advantages: in addition to their all-round availability, they are renewable and, as a rule, ecologically pure low-density materials not requiring disposal after the end of service life. However, being used as such they exhibit a number of disadvantages: low fracture strength and toughness, high brittleness and creep rate [1,2].

Northerners used to strengthen their winter houses made from snow and ice (igloos) with reindeer lichen and moss during many centuries [3]. Systematic engineering-based strengthening of ice was begun about 100 years ago because of the necessity to build winter roads, ferries, floating air-fields, etc. As strengthening additives, wastes of local timber industry (branches, chips, shaving, sawdust) and mineral geomaterials (sand, pebble, crushed stone, alluvium) [4,5] are typically used; under laboratory conditions, natural and synthetic microfibers were used [6–10].

Ice strengthening with macrosize local reinforcing components is intuitively comprehensible, commonly accessible, and raises the ice composite price only scarcely. However, it is subject to a number of restrictions with respect to both the mechanical characteristics and ecology. The experience in using macroadditives and microfibers showed quite soon that the strength of an ice composite with a small content of such components ($\lesssim 3-10$ wt.%, which is relevant to the Arctic) can never be enhanced radically without increasing, in one way or another, mechanical characteristics of the ice matrix itself. However, there is still no system data on the possibilities of ice strengthening due to varying its microstructure by introducing water-insoluble nanoparticles (NP) instead of macrofillers and microfibers or in addition to them. The use of NPs opens prospects for activation of a great number of mechanisms for strengthening the polycrystalline ice matrix (see the discussion at the end of this paper). By now, such a strategy and approaches have never been considered with respect to ice strengthening.

The paper presents the investigation of possibility of the ice matrix strengthening by introducing into distilled water isometric NPs of synthetic silicon dioxide (SiO_2). On the one hand, we have chosen SiO_2 as an inert model material; on the other hand, this material is interesting practically since, for instance, its feedstock (sand, alluvium) is unlimited, ubiquitously available, and ecologically pure.

The ice nanocomposite precursors, namely, suspensions with the SiO_2 NP content c ranging from 0.003 to 10 wt.%, were obtained by introducing in bidistilled water appropriate weighed portions of the SiO_2 nanopowder (Aldrich, USA) whose particle size declared by the manufacturer was $10-20$ nm. The obtained mixtures were processed with ultrasound 100 W in power and 20 kHz in frequency so as to turn them to the state of a stable suspension; for this purpose, probe homogenizer Vibra-Cell VCX 750 (Sonics & Materials, USA) was used. To prevent the suspension heating, the processing consisted in ten cycles 10 s long with inter-cycle intervals of 50 s. Data from scanning electron microscopy showed that the shape of SiO_2 NPs used in preparing the suspensions was almost spherical, and their size was the same as declared by the manufacturer. The ice and ice-composite (IC) samples were prepared in the form of prisms $10 \times 10 \times 20$ mm in size at -10°C in a fridge chamber by using Teflon cuvettes each consisting of 48 individual cells.

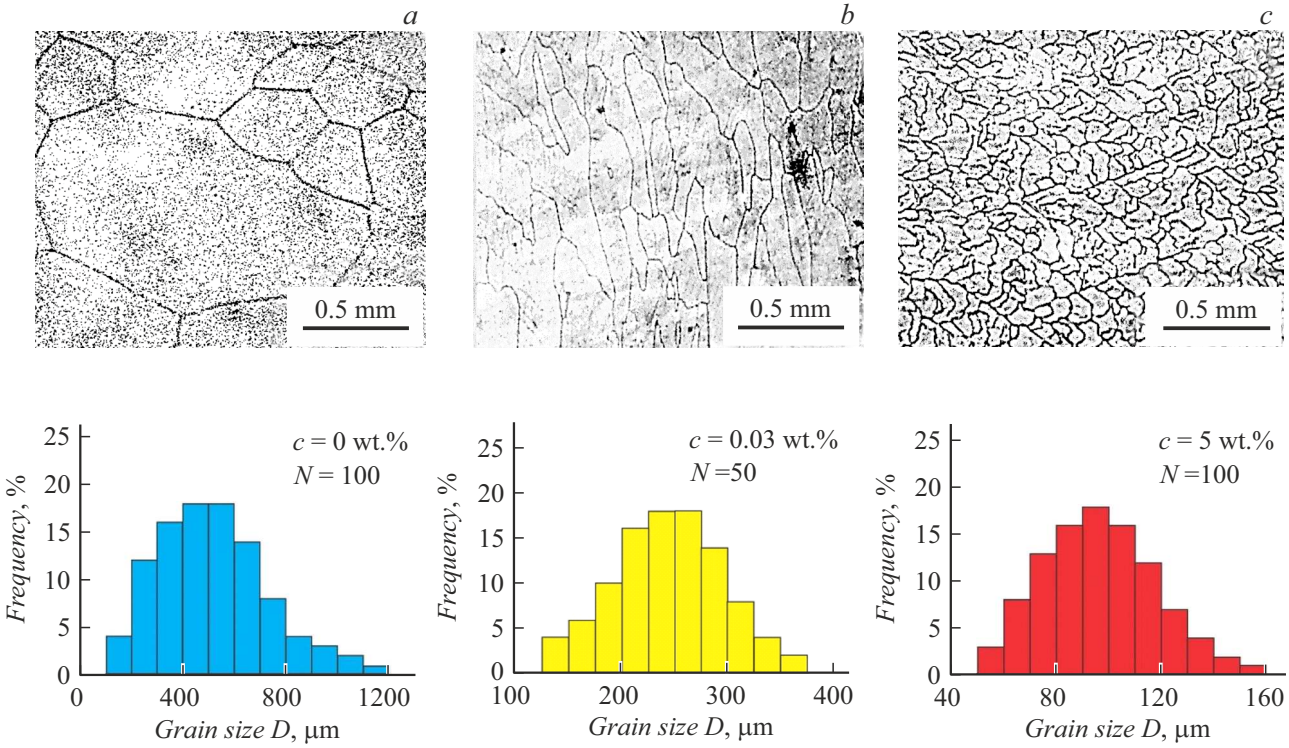

Figure 1. The microsrtructure (top) and grain size distribution (bottom) for pure fresh-water polycrystalline ice and IC versus the silicon-dioxide nanoparticle content in them c. a — pure ice, b — IC ($c = 0.03$ wt.%), c — IC ($c = 5$ wt.%). N is the total number of measured grains.

Microstructures of the ice and IC samples were studied by reflection optical microscopy using an inverted metallography microscope (Axio Observer Carl Zeiss, Germany) equipped with a demountable thermocamera with forced cooling and also with a system of digital acquisition and analysis of images. This allowed studying the microstructure of ice and IC samples at temperature T of down to -50°C. To reveal the grain microstructure, two techniques were used: thermal etching and grain boundary decoration with impurity aggregates.

Mechanical testing of ice and IC by the uniaxial compression method was performed by using servohydraulic test machine MTS 870 Landmark (MTS, USA). It was equipped with a chamber-thermostat (651 Environmental chamber) with the power plunger terminals introduced into its working space. In the experiments, the working space and sample were thermally stabilized by liquid nitrogen vapors supplied from a Dewar vessel. Prior to testing, the chamber working volume was thermostated at a preset temperature. After that, the sample cooled in a refrigerator to the same temperature was placed between the plungers and maintained for 10–20 min in order to equalize all the temperatures in the thermostated volume. Then the samples underwent a mechanical test at $T = -10$°C. The absolute strain rate was 4.8 mm/min which corresponded to the relative strain rate $\dot{\varepsilon} = 4 \cdot 10^{-3}\,\mathrm{s}^{-1}$. The specified values of the sample sizes, T, and $\dot{\varepsilon}$ were chosen just so because they are approximately in the middles of quite broad intervals where the ice strength dependence on these test parameters was weak (or fully absent) [1,2].

Typical optical images of the pure ice and IC microstructures (top row of fragments given in Fig. 1, a–c) show that the IC grain sizes decrease with increasing SiO_2 NP concentration. As known, in the case of crystallization from a large volume of quiet water in the presence of a vertically directed temperature gradient (e.g. during water body freezing), predominantly a columnar grain structure gets formed in ice [1,2,5]. The grains major axes are directed along the temperature gradient (vertically). In this study, just this crystallization thermal mode was realized, except for that the temperature gradient was directed not top-to-bottom as in nature but bottom-to-top, from the cold bottom of the crystallizer towards warm water (the top of the cuvette with cells was heat-insulated). As typical examples of the obtained textures, grain structures transverse to the grains major axes are shown in the Figs. 1, a and c top parts, while Fig. 1, b top part presents the textures along the major axes.

Figs. 1, a–c (the bottom row of fragments) show that in pure ice the grain size distribution (the grain typical size D was defined as an arithmetic mean of two values in mutually perpendicular directions) was characterized by a large width (~ 100 to $\sim 800\,\mu$m) and most probable value $D_m = 500 \pm 50\,\mu$m. Introduction of SiO_2 nanoparticles

resulted in, besides the grain size refinement, in the distribution narrowing due to complete disappearance of grains with $D \gtrsim 400\,\mu$m. For instance, the c increase from 0.03 to 10 wt.% led to the D_m decrease by 2.9 times (from 240 ± 20 to $80 \pm 20\,\mu$m); the decrease with respect to pure ice was 6-fold.

Fig. 2 presents loading diagrams of the pure ice and IC samples with different SiO_2 contents, while Fig. 3 demonstrates the maximal compression stress in the sample σ_{max} versus c in the linear and semi-log scales. Since the magnitude of accumulated strain remains low up to the maximal stresses withstandable by the sample, all the data presented in the plots and in the text are represented in engineering values of stresses and strains. Those figures show that the most significant variation in the IC strength takes place in the c range of 0.01 to 1 wt.%. Therewith, the IC strength increased by 2.5 times. When c continued increasing, the growth of σ_{max} became insignificant; however, by the moment of complete destruction, the energy increased by an order of magnitude, i.e. a brittle-ductile transition took place in the range of SiO_2 $c = 1-10$ wt.%.

Consider possible mechanisms for the observed ice strengthening with SiO_2 nanoparticles. The decrease in the polycrystalline ice grain size with increasing NP concentration is obviously associated with an increase in the number of heterogeneous nucleation centers of crystallites in the sample bulk. Hence, as known, the universal grain-boundary strengthening may be represented by the empiric Hall–Petch relation [1,2]:

$$\sigma_{max} = A + B/D^n, \qquad (1)$$

where A, B and $n \approx 0.5$ may be in the first approximation considered as material constants. Similar relations describe the inhibition of dislocation generation and motion in the basal slip planes due to the disperse strengthening and

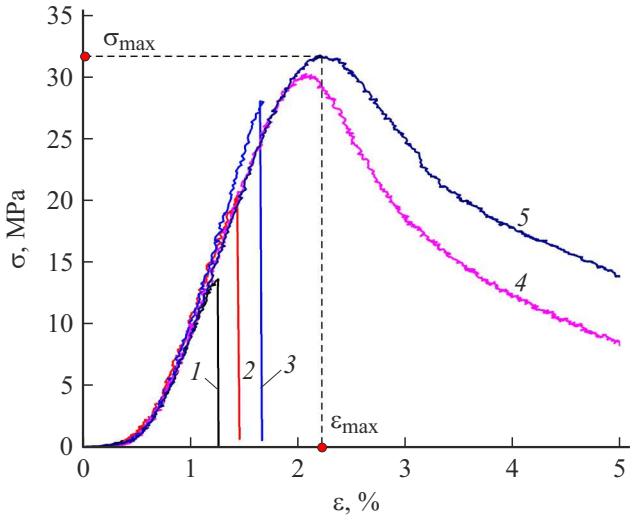

Figure 2. Typical loading diagrams for pure ice (*1*) and IC at $c = 0.1$ (*2*), 1 (*3*), 5 (*4*) and 10 wt.% (*5*). σ and ε are the engineering stresses and strains, respectively.

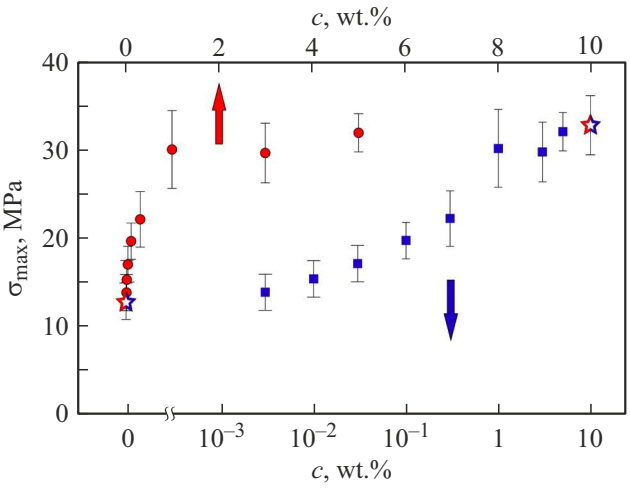

Figure 3. The σ_{max} dependence under the ice-composite uniaxial compression on concentration c of the SiO_2 nanoparticles in the suspension. Asterisks designate common positions of outermost experimental points on the linear and logarithmic scales of NP concentrations: at $c = 0$ wt.% for pure ice and $c = 10$ wt.% for IC.

dislocation cluster penetration through the grain boundary (in this case, n may range from 0.3 to 0.8). Since ices are highly brittle (the pure ice fracture toughness is about an order of magnitude lower than that of silicate glasses), microcracks can arise in them (mainly along the grain boundaries). The most probable length of those brittle microcracks coincides with the grain size, therefore, the decrease in D can result in strengthening according to the Griffiths relation

$$\sigma_{max} = C/D^{1/2}, \qquad (2)$$

where $C = (2E\gamma)^{1/2}$. Here E is the Youngś modulus, γ is the effective surface energy.

To choose between the above-mentioned mechanisms of strengthening with NP, which obey similar relationships, experimental dependence $\sigma_{max} = f(D_m)$ revealed in this study was approximated using the Levenberg–Marquardt algorithm [11] with various test functions. Approximation by relation (1) provides negative values of A with a very large standard deviation ($A = -10 \pm 60$), which is physically senseless (here A is expressed in MPa). Therewith, the final sum of squared residuals is SSR = 47.8. Fixing $A = 0$ and using biparametric approximation, obtain $n = 0.54 \pm 0.07$ at SSR = 48.9. Since the obtained optimal power index n coincides, within the accuracy limits, with the theoretical value 1/2, a biparametric approximation by function (1) with fixed value $n = 0.5$ was carried out. This approximation gave value $A = -2 \pm 3$ at SSR = 48.5, i.e., within the limits of data accuracy and in comparison with σ_{max}, $A \approx 0$. Approximation by one-parametric function (2) (i.e. at $A = 0$) provides SSR = 50.9. The results of the above-described approximations show that, within the experimental accuracy, it is reasonable to assume the relation (1) first term to be negligibly small and power index of D to be close to 1/2. This allows concluding that the predominant process

limiting the strength of tested ice and IC samples is the microcracks generation and development over the grain boundaries.

Thus, the study has shown that adding to ice high-disperse (10−20 nm) SiO_2 nanoparticles in the amount of up to 10 wt.% causes six-fold reduction of the mean grain size and ice composite strengthening by 2.5 times in the uniaxial compression test. The fastest strength increment (up to 2 times) takes place in the range of SiO_2 nanoparticle concentration of 0.01 to 1 wt.%.

By comparing the accuracy of the experimental data approximation by the Levenberg−Marquardt technique via the Hall−Petch and Griffith formulae, it was shown that, most probably, the predominant strengthening mechanism is a decrease in length of the Griffithś intergrain cracks caused by a decrease in the grain mean size with increasing NP concentration. More detailed revealing of micromechanisms for modifying mechanical characteristics of ice and IC with the aid of high-disperse NPs, as well as of their strengthening potential, needs system experimental research using NPs of different natures, morphologies, sizes and concentrations. Such researches will be performed in the nearest future; this will allow adding to the range of conventional techniques for ice strengthening with macrocomponents and microfibers a set of new methods and means for modifying mechanical properties of the ice matrix itself.

Acknowledgements

The results were obtained by using equipment of the G.R. Derzhavin TSU Common Use Center.

Financial support

The study was supported by the Russian Science Foundation (project 22-19-00577).

Conflict of interests

The authors declare that they have no conflict of interests.

References

[1] L.U. Arenson, W. Colgan, H.P. Marshall, in *Snow and ice-related hazards, risks, and disasters* (Elsevier Inc., 2015), p. 35–75. DOI: 10.1016/B978-0-12-394849-6.00002-0
[2] E.M. Schulson, P. Duval, *Creep and fracture of ice* (Cambridge University Press, Cambridge, 2009).
[3] A. Pronk, N. Vasiliev, J. Belis, in *3rd Int. Conf. on structures and architecture (ICSA 2016)* (CRC Press Taylor & Francis Group, London, 2016), p. 339–347.
[4] N.R. Vasiliey, A.D.S. Pronk, I.N. Shatalina, F.H.V.T. Janssen, R.W.G. Houben, Cold Reg. Sci. Technol., **115**, 56 (2015). DOI: 10.1016/j.coldregions.2015.03.006
[5] F.H.M.E. Janssen, R.W.G. Houben, *Reinforced ice structures* (Eindhoven University of Technology, Eindhoven, 2013).
[6] G.A. Nuzhnyi, V.M. Buznik, D.V. Grinevich, D.N. Landik, R.N. Cherepanin, Inorg. Mater.: Appl. Res., **11** (1), 103 (2020). DOI: 10.1134/S207511332001027X
[7] Y. Wu, X. Lou, X. Liu, A. Pronk, Mater. Struct., **53** (2), 29 (2020). DOI: 10.1617/s11527-020-01463-2
[8] X. Liu, Y. Wu, Cold Reg. Sci. Technol., **192** (2), 103381 (2021). DOI: 10.1016/j.coldregions.2021.103381
[9] X. Lou, Y. Wu, Cold Reg. Sci. Technol., **194**, 103458 (2022). DOI: 10.1016/j.coldregions.2021.103458
[10] J. Xie, M.-L. Yan, J.-B. Yan, Cold Reg. Sci. Technol., **206**, 103751 (2023). DOI: 10.1016/j.coldregions.2022.103751
[11] W.H. Press, S.A. Teukolsky, W.T. Vetterling, B.P. Flannery, *Numerical recipes in C: the art of scientific computing*, 2nd ed. (Cambridge University Press, Cambridge, 1992).

Translated by Solonitsyna Anna